Research methods

A method for measuring systolic and diastolic microcirculatory red cell flux within the canine myocardium

Katherine D. Barclay, Gerald A. Klassen*, Rene W.G. Wong**, Alan Y.K. Wong***

*Department of Physiology and Biophysics, Dalhousie University, Halifax, NS, *Division of Cardiology, Queen Elizabeth II Health Sciences Centre, and Departments of Medicine, and Physiology and Biophysics, Dalhousie University, Halifax, NS, **Medical Student at Dalhousie University, Halifax, NS, ***Department of Physiology and Biophysics, Dalhousie University, Halifax, NS, Canada*

Key words:
Coronary microcirculation; Laser Doppler velocimetry; Red cell flux.

Background. **Knowledge of the patterns of movement of red cells during the cardiac cycle in the microcirculation within the contracting myocardium is largely unknown. We describe a method of making such measurements in the canine myocardium using the technique of laser Doppler velocimetry.**

Methods. **A lensed 100 µm fiber-optic probe was inserted into the beating myocardium at various sites. Using an ultra-stable laser and achieving measurement stability by heterodyning the laser light and reflected light from the tissue, it was possible to obtain a stable high quality measurement of predominately red cell movement in the microcirculation.**

Results. **Unique regional patterns of red cell movement within the myocardium were observed. Epicardial flux was continuous with peaks while endocardial flux was predominately diastolic. Stopping flow in the epicardial artery for 5-6 s demonstrated that red cell movement continues in the microcirculation with some reduction followed by a delayed reactive hyperemia. Modeling demonstrates an important role for the small coronary veins in control of microcirculatory red cell movement.**

Conclusions. **It is possible using laser Doppler velocimetry to measure red blood cell flux in the beating canine myocardium. Such measurements demonstrate a high degree of complexity which is not reflected in epicardial coronary arterial or venous flow.**

(Ital Heart J 2001; 2 (10): 740-750)

This work was supported by a grant from the Heart and Stroke Foundation of Nova Scotia. A contribution towards the equipment used to make the measurements was provided by the Dalhousie Medical Research Foundation.

Received May 28, 2001; revision received August 27, 2001; accepted August 30, 2001.

Address:

Dr. Gerald A. Klassen

137 Newcombe Branch Road
RR #2
Centreville, NS B0P 1J0
Canada
E-mail: gklass@ns.sympatico.ca

Introduction

Oxygen delivery to the cardiac myocyte depends upon the physical forces governing the passage of red cells through oxygen exchanging arterioles and capillaries during the cardiac cycle. The hemodynamics of the coronary microcirculation remains largely unknown[1]. Direct observation using microscopy of epicardial and endocardial surface capillaries has provided some information concerning red cell flow during the cardiac cycle[2-5]. However, restraining devices required to make such observations may introduce artifacts by inhibiting systolic forces[6]. We have developed methodology based upon laser Doppler detection of red blood cell (RBC) velocity (flux) which allowed us to measure myocardial microcirculatory RBC flux during systole and diastole lessening restraint artifacts in the beating rabbit heart[7]. Data from the rabbit myocardium demonstrated that red cells move continuously throughout the cardiac cycle and that there were usually two or three peaks of accelerated RBC flux. However, it was not possible to correlate microcirculatory events with large epicardial vessel flow because the small size of the rabbit coronary arteries and veins precluded the use of flowmeters.

In this study in the dog we measured RBC flux using the laser Doppler velocimeter[7] concurrently with epicardial coronary arterial and venous flows as measured by ultrasonic transit-time flow probes and left ventricular pressure. This device measures the velocity of red cells within a small area of the microcirculation (5 capillaries in diameter and 1-2 capillaries in depth). It aggregates all velocities and does not differentiate forward from reverse flow. Multiple sites in the myocardium were selected for RBC flux measurements. We examined the stability of the RBC flux signal over time. We also recorded the response to a 5-6 s coronary arterial occlusion and the subsequent reactive hyperemia. A short period of arterial occlusion was selected as a stimulus for increasing coronary blood flow. Such a short duration of occlusion in-

duces minimal myocardial ischemia. Finally, the data were modeled to determine which parameters present in the coronary arterial and venous flow signals were predictors of the systolic/diastolic pattern of RBC flux within the contracting myocardium.

Methods

Measurement of systolic/diastolic microcirculatory red cell flux. The laser Doppler technique allows for the measurement of particle velocity using the Doppler principle. The laser Doppler velocimeter used was designed in our lab and consisted of an ultra-stable, long cohesion 3.2 mW helium-neon laser (Laboratory for Science, Berkeley, CA, USA) with a wavelength of 632.8 nm, a lensed fiber-optic probe, a light detector and a signal processor. Light from the laser is passed through an optical cable to a coupler where it is split in a 9:1 ratio; 90% of the light continues through a connector to the fiber-optic probe while 10% is directed back to the detector to correct for variation in the laser's output. The single fiber-optic probe supplies the input reference light and returns both the reflected non Doppler shifted (reflected by non moving structures) and Doppler shifted light (caused by the movement of primarily the RBC in tissue) back to the detector. This device has been described previously[7]. Briefly, the laser light (frequency ~5 $\times$ 10^{14} Hz) travels down the optical fiber into the tissue where it is Doppler shifted largely by the moving RBCs. The light scattering by moving particles imparts a Doppler shift to the light such that the frequency can be shifted by values of 500-5000 Hz (in tissue typically by 3000 Hz). The Doppler shifted light travels back through the fiber to the coupler where it passes into another fiber connected to an avalanche photodiode. Backscattered light due to the differing indices of refraction between glass and tissue and unscattered light reflected from the tip of the optical fiber also travels to the detector but is of negligible magnitude. The Doppler shift depends upon the velocity of the RBC as well as the cosine of the angle between the light scattering vector and the RBC velocity vector. Because each scattering by a moving particle can impart a different frequency shift depending upon the velocity vector and the vector of the scattered light, a broad spectrum of Doppler shifts is recorded.

The dominant particle moving through tissue with a velocity giving rise to a spectral shift will be the red cell. Slow moving white cells or platelets which are few in number will contribute minimally. Because of the size of our probe tip (100 μm) the dominant vessels which will be observed will be those of the microcirculation. Measuring the direction of blood flow is not possible with our laser Doppler device. Direction detection requires spectral analysis which needs a larger signal-to-noise ratio than was available. In the beating myocardium, microvessels form a network in which RBC move in many directions but always from arterioles to venules as the system is closed. Our device is advantageous compared to laser Doppler devices designed to measure particle flow in a single vessel. Our device produces a composite of all RBC velocity vectors and scattering vectors reflected into the probe tip. Because the particle vectors are aggregated by the device it is number- (hematocrit) and velocity-dependent. Hence we have used the word RBC flux to describe the resultant values. The volume of tissue observed is in the order of ~5.5 $\times$ 10^{-5} mm^3 (in the shape of a truncated cone) (Fig. 1). This region of interest was calculated by assuming the field of observation was 100 μm in diameter spreading with a 12 degree divergence. A depth of penetration of 7 μm was assumed from measurements made in our laboratory and from literature values reported for this type of laser[8]. Laser Doppler flowmeters that measure blood flow direction by spectral analysis have an advantage where particle numbers are high and blood flow is either fully forward or fully reversed such as flow in a coronary artery or vein, but not in a vascular network where such organized flow does not occur.

The fiber-optic probes used were multi-mode with a diameter of 100 μm and covered with a plastic cladding so that total external diameter was 140 μm. They were made to our specifications by Focal Technologies, Inc. (Dartmouth, NS, Canada). One end of the fiber consist-

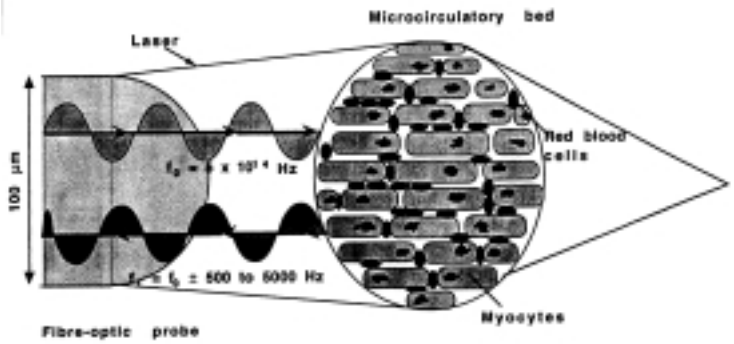

Figure 1. *Diagram of laser Doppler sensing of red blood cell flux. The lensed fiber-optic probe delivers monochromatic light to a flat truncated cone of functional myocardium. The movement of the particles (red blood cells) phase shift the input frequency according to their velocity. The Doppler shifted light returns to the detector (avalanche photodiode) via the fiber and the input and output (tissue) frequency form a "beat" frequency which results in a root mean square voltage which is proportional to the velocity and number of moving particles in the field.*

ed of a fiber collimator connector. At the other end a section of 1 cm of the plastic cladding was stripped from the fiber and a lens formed on the bare tip using a fusion splicer (Model PFS101, Foundation Instruments, Ottawa, ONT, Canada). The lens allows for dispersal of the laser light at an angle of approximately 12 degrees. Calibration of each fiber-optic probe within a flowing fluid medium, was done using a milk solution and a calibrated pump. It was found that for our system, a linear increase in the velocity at which the milk was pumped through tubing in which the probe was present resulted in a linear increase in RMS voltage up to a maximum velocity of 30 cm/s. Zero RBC flux was measured in the non beating heart at the end of each experiment and subtracted from the recorded values[9,10]. This measurement corrects for tissue reflectance from non moving particles.

Animal preparation. Fifteen mongrel dogs (10 females and 5 males) with a mean weight of 18 ± 1 kg constituted the study group. The investigation conforms with the Guide for the Care and Use of Laboratory Animals published by the US National Institutes of Health (NIH Publication No. 85-23, revised 1985). The animals were anesthetized with sodium thiopental (25 mg/kg, Abbott Laboratories, Montreal, QC, Canada), intubated and maintained on a respirator (Mark 7A, Bird Corporation, Palm Springs, CA, USA). Body heat was maintained at 37°C with a heated water blanket. The chest was opened through a bilateral thoracotomy and then the anesthetic was changed to α-chloralose (50 mg/kg, Sigma Chemical Co., St. Louis, MO, USA). The pericardium was opened and a pericardial cradle formed for the heart. A 5F catheter pressure transducer (Medical Measurements, Inc., Hackensack NJ, USA) was introduced into the left ventricle via the apex for measurement of left ventricular pressure. A small section of the proximal left anterior descending coronary artery (LAD) was dissected free and an ultrasonic Doppler transit-time flow probe (model 2RS, Transonic Systems, Inc., Ithaca, NY, USA) was placed for measurement of coronary arterial flow. In 5 dogs, a small section of a distal cardiac vein adjacent to the LAD and proximal to the great cardiac vein was isolated and a second Doppler transit-time flow probe was placed for measurement of coronary venous flow. In 1 dog, a second flow probe was placed, distal to the first probe, on the LAD. It should be noted that this device measures both red cell and plasma velocity in a volume so that total blood flow during the cardiac cycle is recorded. It is not sensitive to changes in hematocrit. This is in contrast to the fiber-optic laser Doppler velocimeter (FOLDV) which records RBC flux and not non particle plasma flow.

Insertion of the probe into the beating heart. A 20G, plastic intravenous catheter with an inner needle (Critikon, Tampa, FL, USA) was threaded along the myocardium, for at least 1 cm, the inner needle removed and the external plastic catheter left in place as a guide for insertion of the FOLDV probe. The depth of placement of the needle differed for each dog with locations ranging from epicardium to endocardium. The usual site was adjacent to the LAD, distal to the flowmeter. In 2 animals, the probe was subsequently inserted into the upper septum and the apex. In 1 animal, the probe was also inserted into the right ventricular wall and the right atrium. The FOLDV probe was inserted through the plastic needle and then the sheath was withdrawn so that the probe was held in place by the contracting myocardium. Virtually no tethering of the myocardium took place. The probe was held in place by the traversed contracting muscle and was not anchored to the epicardium. The signal was not sensitive to the bending motion of the fiber by the beating heart. The success of our system to measure microcirculatory red cell flux relates to both the method of measurement as well as to the minimal mass of the fiber. If the fiber moves relative to the vascular bed such movement will introduce a Doppler shift artifact. By inserting the fiber so that it was anchored by the surrounding myocytes we achieved our goal. If hemorrhage occurs with thrombus formation at the tip (confirmed by histology) the signal ceases, confirming that moving RBCs and not movement artifact of the fiber by the muscle gave rise to the signal. The signal was much reduced in infarcted myocardium. After the completion of the study the animal was euthanized using a large dose of barbiturate. Baseline correction for RBC flux was measured when all cardiac action ceased.

The pressure transducer, transit-time flow probes, electrocardiogram and FOLDV were connected to a data acquisition system (MP100, BIOPAC Systems, Inc., Goleta, CA, USA) and then to a Macintosh PowerBook Duo 270c. Data was sampled at 500 Hz and acquisition was controlled using the BIOPAC software, AcqKnowledge III.

Experimental procedure. *Control.* After instrumentation, control readings were taken for electrocardiogram, left ventricular pressure, coronary arterial and venous blood flow and myocardial tissue RBC flux until steady state was apparent. Data were continuously acquired throughout the experiment and all parameters were allowed to return to control values before the next intervention was applied.

Reactive hyperemia. To test reactive hyperemia, the isolated LAD was occluded, by digital pressure, for a period of 5-6 s in 9 dogs. Because of their close proximity the epicardial coronary veins adjacent to the artery were frequently occluded. In one instance, following 10 μg of angiotensin II given into the left atrium a spontaneous stop flow of ~29 s was observed in the FOLDV signal. It was followed by typical reactive hyperemia. The event was not apparent in the coronary arterial or left ventricular pressure tracings. We termed this microvascular spasm. Repeated injections of the

same drug in this animal and in others failed to reproduce the microcirculatory event.

Signal processing. *Data smoothing*. For purposes of graphing, the data from the laser Doppler velocimeter were smoothed using the formula:

$$f_{output}(n) = \Sigma\, f_{input}(k) \quad [1]$$

where Σ is from $k = n - (m\ 2^{-1})$ to $k = n + (m\ 2^{-1})$ and m is the number of points in the window and n is the sample number.

Means. Mean values for the tissue RBC flux, coronary artery flow curves and coronary venous flow curves (where applicable) were measured from beat-to-beat data using the AcqKnowledge III program. The following formula was applied:

$$\bar{X} = 1/n\Sigma X_j \quad [2]$$

where Σ is from j = 1 to n (AcqKnowledge III for the MP100WS hardware and software reference manual, BIOPAC Systems, Inc., Goleta, CA, USA, 1993).

Results

Relationship of red blood cell flux to the cardiac cycle. Figure 2 demonstrates the relationship of the red cell flux in the microcirculation to left ventricular pressure and coronary epicardial arterial and venous flow. The recording site was superficial, adjacent to the LAD. Red cell flux was continuous with three peaks. The first peak coincided with isovolumetric systole (peak 1), the second with isovolumetric diastole (peak 2), and the third diastole (peak 3). This pattern was representative of the superficial region of the free wall of the left ventricle. Peak 2 during late systole coincides with peak venous outflow, while peak 3 (early diastole) with peak arterial inflow.

Figure 3 is a composite of representative RBC flux from different locations in the myocardium.

Deep myocardium (Fig. 3A). The site for recording was deep in the free wall of the left ventricle adjacent to the LAD. In contrast to figure 2 (superficial) there are only two peaks. Both peaks are diastolic, one early and the second late. Systolic microcirculatory RBC flux is decreased and reaches a nadir during late systole.

Apex (Fig. 3B). The device was placed so that its tip was within myocardium at the apex. As the myocardium is relatively thin at this site the position was easily ascertained from transillumination by the laser. Figure 3B demonstrates a representative pattern. Three large peaks were observed: two in diastole and the third in early systole. Minimal RBC flux occurred during peak systole through to diastole. The apex and the superficial region of the left ventricle both had three peaks but the RBC flux pattern of the apex was different being predominately diastolic and, in that respect similar to the deep myocardium.

Septum (Fig. 3C). The optical fiber was threaded so that the tip was in the anterior superior portion of the muscular intraventricular septum. The RBC flux pattern had two peaks, all within the envelope of epicardial coronary arterial flow (diastolic). Minimal flux was present during peak systole.

Right ventricle (Fig. 3D). The probe was placed in the free wall of the right ventricle. Two peaks were recorded of RBC flux, one during isovolumetric systole and the second during isovolumetric diastole. RBC flux reached nadirs twice, once during peak systole and again during diastole.

Right atrium (Fig. 3E). The probe was threaded along the posterior wall of the right atrium where a stable

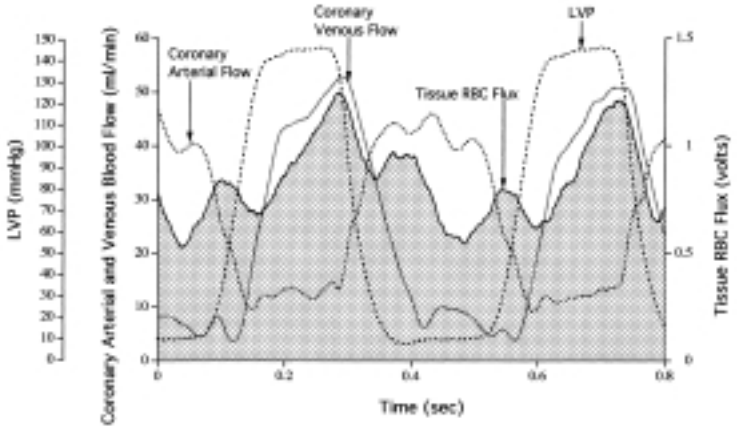

Figure 2. *Recording of two cardiac cycles of red blood cell (RBC) flux from a typical superficial region of the myocardium adjacent to the left anterior descending coronary artery measured in volts. Simultaneous measurements of epicardial coronary arterial flow (proximal) and coronary venous flow (distal) as measured by an ultrasonic transit-time flowmeter and left ventricular pressure (LVP) are demonstrated.*

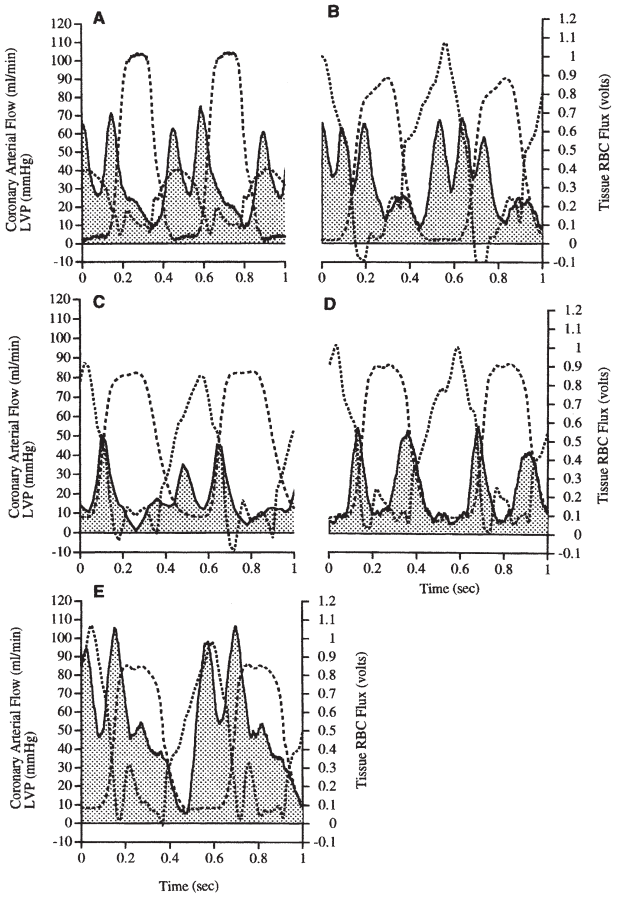

Figure 3. *Representative regional patterns of RBC flux are illustrated. Sites are* A: *deep myocardium adjacent to the left anterior descending coronary artery;* B: *apex;* C: *superior portion of muscular intraventricular septum;* D: *free wall of the right ventricle;* E: *right atrium, muscular portion.* B-E *were recorded in the same animal. RBC flux is indicated by the shaded area. LVP* (dashes) *and left anterior descending coronary artery flow* (dots) *are illustrated for two cycles. Abbreviations as in figure 2.*

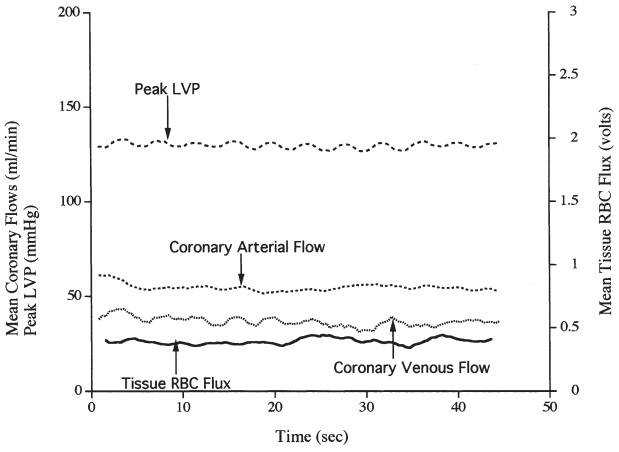

Figure 4. *Control measurements before interventions. Measurements are* from top to bottom: *peak LVP, highest LVP per beat, mean epicardial coronary arterial flow, mean epicardial coronary venous flow, and mean tissue coronary RBC flux. Abbreviations as in figure 2.*

position could be found in this thin-walled structure (probably in Bachmann's bundle). Red cell flux had two prominent peaks which coincided with coronary arterial flow during diastole and the isovolumetric period of ventricular systole. The first peaks coincide with the period of atrial systole. The nadir for RBC flux was during the initial phase of ventricular diastole.

Stability of red blood cell flux over time (Fig. 4). The stability of red cell flux pattern over time was measured for up to 30 min without an intervention. As long as coronary arterial flow and left ventricular pressure were constant no alteration in either the pattern or mean value of RBC flux occurred. In some animals a respiratory variation in the pattern of flux was observed. When the preparation began to deteriorate after 3 to 4 hours of interventions, the magnitude of RBC flux appeared to be the initial parameter to decrease before changes in epicardial arterial coronary flow or left ventricular pressure. Figure 4 demonstrates mean arterial and venous flow, RBC flux and peak left ventricular pressure for 30 s while no interventions occurred. Such a duration of constancy was observed before interventions were applied.

Stop flow and reactive hyperemia (Fig. 5). When a brief 5-6 s coronary arterial occlusion was performed the typical arterial response was observed. In 9 dogs in which a control stop flow intervention was performed with measurement of RBC flux in the region of the myocardium supplied by the occluded artery (5 superficial, 3 deep and 1 in the mid myocardium) no typical response was observed. Figure 5 demonstrates the pattern of RBC flux (FOLDV) in the mid myocardium before, during and after a short period of coronary arterial occlusion. Following occlusion there is a minimal increase in RBC flux. Left ventricular pressure decreases during occlusion and then returns to control. Coronary artery flow (LAD flow) is minimal during occlusion, and demonstrates, following release, an impressive reactive hyperemia. No significant changes in the systolic/diastolic flow pattern of the RBC flux were observed in this animal.

In most instances during reactive hyperemia there were only minor changes in the systolic/diastolic RBC flux pattern. In one instance while mechanical alternans was present, both the epicardial coronary arterial flow pattern and the RBC flux demonstrated alternans. During the initial period of reactive hyperemia the alternans pattern decreased in all measurements. When the epicardial artery was occluded, at no time (except following a short period of asystole associated with an arrhythmia) did RBC flux fall to zero as did arterial and venous flows. During occlusion diastolic RBC flux was usually decreased. No other consistent changes in the systolic/diastolic flow pattern emerge from this set of observations.

In some instances the reactive hyperemia pattern was delayed compared to the arterial pattern. If the length of

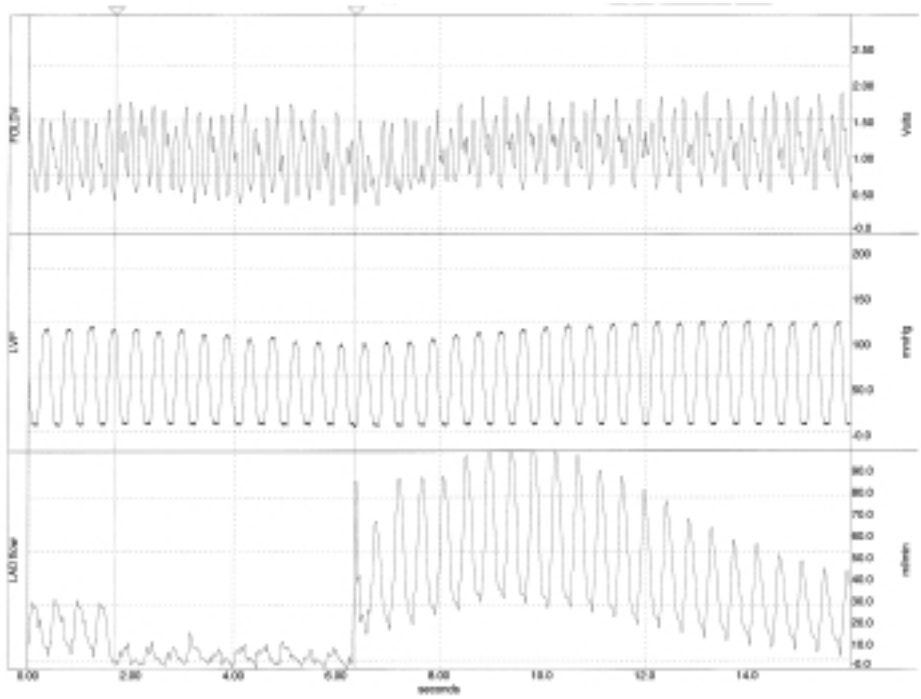

Figure 5. *Record of coronary arterial stop flow (5 s). The onset and offset are marked by* arrows *and* lines. *Red cell flux (fiber-optic laser Doppler velocimeter-FOLDV) in mid myocardium in distribution of the left anterior descending coronary artery (LAD). Left ventricular pressure (LVP) and LAD flow are presented in the* middle *and* lower panel *respectively. Note marked arterial hyperemic response in the presence of minimal red cell flux changes.*

the hyperemic response was considered in those where it could be reliably measured (n = 4), the average duration of hyperemia in the artery was 10 ± 2 s while in tissue the response was longer (19 ± 2 s, p = 0.02).

Microvascular spasm (Fig. 6). A spontaneous 29 s stop flow, in only the FOLDV signal is illustrated in figure 6. During the period of arrested flow, low voltage systolic oscillations were observed consistent

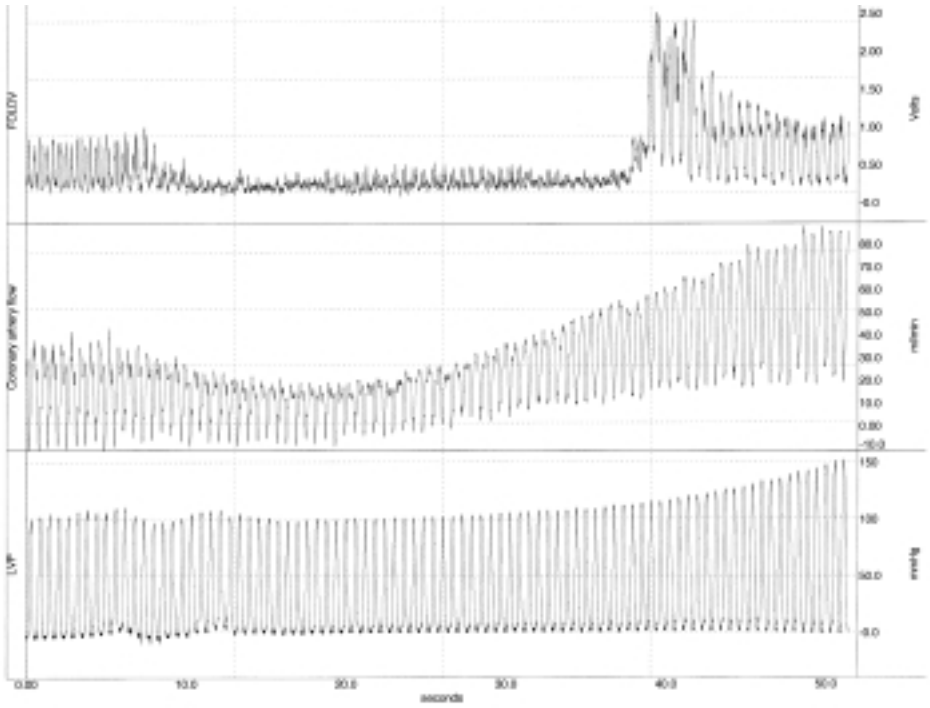

Figure 6. *A demonstration of spontaneous microvascular spasm followed by a reactive hyperemia. Record of red cell flux (FOLDV), deep epicardium in the distribution of the LAD, coronary arterial flow and LVP. At the onset of the recording 10 μg of angiotensin II was administered as a bolus into the left atrium. Abbreviations as in figure 5.*

with minimal RBC flux. A 3-fold increase in RBC flux was observed during peak reactive hyperemia when comparing control RBC flux (before angiotensin II) to peak flux hyperemia. Left ventricular pressure did not change during the period of reduced RBC flux. Coronary arterial flow following angiotensin II administration demonstrated a decrease in LAD flow followed by a gradual increase above control. The FOLDV event could not be detected from the concurrently measured left ventricular pressure and LAD flow, hence we termed this event microvascular spasm. The coronary flow and left ventricular pressure responses are typical of observed responses to this dose of angiotensin II.

Discussion

Measurement of coronary microcirculatory blood flow has been fraught with technical difficulties. It has long been recognized[11] that the primary control of the coronary circulation must lie at this level (i.e., the myocyte-microcirculatory relationship for oxygen delivery). Tillmanns et al.[3] exploited rapid capillary cinematography with restraining devices to measure red cell movement in surface capillaries of the myocardium and in the left atrium using transillumination. They demonstrated both systolic and diastolic RBC movement. Ashikawa et al.[4] using a "floating microscopic" approach advanced this methodology and demonstrated that capillary RBC flow in surface epicardial and endocardial capillaries was almost continuous with a nadir during isovolumetric systole. Yada et al.[5] using videomicroscopy have examined reactive hyperemia in the subendocardium. Chilian[1] has recently summarized attempts to make such measurements. Others have attempted to use the laser Doppler technique for detecting red cell movement in the myocardium but have found that movement artifact of the tip of the probe relative to the microvasculature precluded accurate measurement of RBC flux in the untethered myocardium[12,13]. We have recently reported[7] results of measurement of RBC flux in the rabbit heart where we were able to overcome the technical problem of making such measurements. In this manuscript we are reporting observations of the coronary microcirculation in the canine heart during the cardiac cycle where it was possible to measure epicardial coronary arterial and venous blood flow simultaneously.

During control conditions in the canine heart, as in the rabbit myocardium, superficial tissue RBC flux is continuous throughout the cycle but with three peaks: one during isovolumetric systole, a second during isovolumetric diastole and a third diastolic peak. These results differ from Ashikawa et al.[4] who detected flow reversal in larger microvessels at the onset of isovolumetric systole. However, their and our results are in agreement in that the major component of red cell movement occurs during both systole and diastole as had been previously described using less sophisticated technology by Tillmanns et al.[3] for both the dog and turtle epicardial capillaries. It is possible that the restraining devices used by Ashikawa et al.[4] contributed to the apparent flow reversal. Our data suggest that at least one velocity peak is related to venous outflow, the second to coronary arterial inflow, and the third could be related to intravascular compliance changes occurring during isovolumetric systole – a period of shape change for the myocardium. A possible explanation for this pattern will be presented in the "model section".

There has been considerable speculation concerning the pattern of endocardial blood flow during the cardiac cycle based upon the observation that when perfusion pressure is reduced subendocardial ischemia ensues[14]. It was concluded that such flow would be predominately diastolic. Our data confirm this. Phasic flow predominates with two prominent peaks – both during diastole.

Interest in apical perfusion has been enhanced by the appreciation of the region's unique mechanical twisting motion during systole[15]. Like the endocardium, RBC flux was mainly diastolic with two peaks but there was an additional third peak during early systole. In addition, RBC cell flux was delayed compared to coronary artery inflow. This raises the possibility that the length of coronary artery and its branching pattern as elucidated by Zamir[16] may have an effect on the pattern of tissue red cell flux in a region.

The ventricular septum is of interest given that the coronary arterial input has been recognized to be unique with a period of flow reversal during early systole. Tissue RBC flux was minimal during peak systole when red cell movement all but ceased. Epicardial flowmeters demonstrate that the septal artery has mainly diastolic flow[17]. Similar to the apex, diastolic flow peaks were delayed compared to arterial inflow.

The right ventricle with its thinner wall and lower developed cavity pressure demonstrated both lower total RBC flux and a pattern of RBC flux occurring during periods of shape change (i.e., isovolumetric contraction and relaxation). Presumably these would be the periods of highest oxygen requirement for the myocytes and the RBC flux pattern which may reflect the more ideal conditions for perfusion which this chamber enjoys.

Kajiya et al.[18] used laser Doppler to detect RBC flux within small surface arteries and veins of the atrium. Hellberg et al.[2] reported observations of atrial capillary RBC velocity in the microcirculation of the left atrial appendage using cinematography. Hellberg's reported pattern was similar to the RBC flux pattern in figure 3D (i.e., peak velocity during late diastole and early systole). This pattern coincides with the period of atrial activation and recovery and is sim-

ilar to the pattern of apical RBC flux. It should be noted that the right atrium is functionally and anatomically heterogeneous[19].

We have published regional patterns of RBC flux in the rabbit heart[7]. Heart rates were lower in the dog; nevertheless, the regional patterns are remarkably similar. For example, the nadir of RBC flux in the septum and apex during mid systole is similar. Measurements of right ventricular and right atrial RBC flux were not performed in the rabbit. It was not necessary to leave the pericardium intact in the dog heart, in contrast to the rabbit, to obtain stable recordings of RBC flux.

What physiologic purpose could be served by having two-three peaks of RBC flux during each cycle? Given the maximal degree of oxygen extraction which occurs in the myocardium, it would facilitate the exposure of oxygenated erythrocytes to myocytes by imposing a number of periods of rapid movement of RBCs (removing oxygen-spent RBCs) with slower ones (allowing time for oxygen extraction)[20].

Recently Kuznetsova et al.[21] have compared microsphere measurements for blood flow with laser Doppler in resting rat skeletal muscle in the presence of vasodilators and found poor agreement. This is not surprising given that, in the presence of vasodilators, changes in tissue hematocrit can occur as red cell transit-time and plasma transit-time diverge[22]. As well, blood cells such as erythrocytes and leukocytes contribute to blood flow resistance in the microcirculation through being deformable and folding as they traverse capillaries which are similar or smaller in diameter[23]. Microcirculatory flow as measured by microspheres should be considered as a static snapshot of arteriolar flow, being rigid they are not amenable to passage through capillaries and neither reflect the passage of deformable erythrocytes in the microcirculation nor the variable transit-times of plasma and blood cells as tissue hematocrit changes.

Arterial stop flow and reactive hyperemia. The continuous movement of RBC in the microcirculation during the duration of coronary arterial occlusion was observed. Our device does not register the direction of RBC flux (i.e., the RBC may be moving back and forth so that oxygen delivery is no longer occurring). This observation emphasizes that an important component of capillary RBC flux may be contributed to by the contraction of the myocyte. Minor changes in the FOLDV pattern (Fig. 5) are observed concurrent with arterial occlusion. The physiology of the response of the coronary circulation to a brief arterial occlusion has been reviewed by Olsson[24]. This maneuver has been widely applied as a tool to evaluate the extent of obstruction to coronary arterial flow (coronary flow reserve) in patients with stenotic coronary arteries with variable success[25]. As Olsson indicates in his review, the response of reactive hyperemia is more complex than simply an increase in flow resulting from ischemic dilation of the vessels in the myocardium engendered by an arterial occlusion. Information concerning microcirculatory RBC flux during epicardial vessel occlusion and reactive hyperemia has not been available: therefore our results are unique and somewhat surprising. One would expect that abrupt arterial occlusion would result in a delayed precipitous drop in RBC flux in tissue. A factor contributing to the lack of response of RBC flux to arterial occlusion may be both the short duration of occlusion and the adequacy of collaterals to the capillary bed under observation[26]. Nevertheless, an epicardial arterial reactive hyperemia was induced. Since the volume of the myocardium under observation is small (5 capillaries in diameter and 1-2 capillaries in depth) there is probably a heterogeneous capillary response to the intervention. Since a change in the RBC flux occurred during epicardial arterial occlusion the minimal changes observed while the arterial hyperemia is present may be appropriate for the microcirculation, as little global evidence of ischemia was observed. This would suggest that a component of the epicardial arterial hyperemia response was secondary to the mechanics of vessel occlusion rather than ischemia, a possibility suggested by Olsson[24]. The blunting and delay of the hyperemic response in the microcirculation and not in the coronary artery or vein would be in agreement with Spaan et al.'s[27] proposal of a large intramyocardial vascular compliance. It is also consistent with our previous report of a large intramyocardial blood volume as measured by indicator dilution in patients[28]. Another factor which must be considered to explain our observations would be a change in tissue hematocrit. Ruiter et al.[29] demonstrated that during reactive hyperemia coronary sinus oxygen saturation increases markedly, consistent with either opening of arterio-venous RBC shunts or a very rapid capillary transit-time[20] as occurs when some coronary vasodilators are given. The FOLDV measures only RBC flux and not plasma flow while the transit-time flowmeter measures both. Olsson[24] had proposed that a regional discrepancy in the pattern of systolic/diastolic blood flow during reactive hyperemia might occur, particularly an increase in systolic epicardial flow. Our results do not exclude this possibility. Our small sampling volume and spatial tissue flow heterogeneity may account for the variable responses to arterial occlusion we observed[30]. The complexity of interactive controls for RBC flux in the microcirculation[22] make the use of a stop flow and consequent reactive hyperemia to calculate coronary flow reserve a problematic exercise. It is probable that as the duration of arterial occlusion increases, regional ischemia increases and myocyte function is depressed. Therefore the to-fro augmentation of RBC flux by myocyte contraction may decrease. This was not tested.

Microvascular spasm. The serendipitous unique occurrence of a 29 s episode of minimal RBC flux, perhaps related to angiotensin II administration, but involving only a portion of the microcirculation, demonstrates that the microcirculation can respond with a typical reactive hyperemic response. Where this spasm occurred, small artery, arteriole, capillary or a combination is unknown. The occlusion was sufficient that capillary RBC flux was essentially arrested, either because of a localized decreased myocyte function, or the spasm site was distal to the entry point of collaterals, or a generalized decrease in microcirculatory lumen size inhibited RBC movement. During hyperemia the peak integrated RBC flux increased approximately 3-fold and was followed by damped oscillations in RBC flux. While it would be tempting to claim that this is analogous to microvascular spasm as is suggested to occur in syndrome X there is no convincing evidence to do so.

Modeling of tissue red blood cell flux. Because of the many factors which could influence RBC flux at a microcirculatory level during the cardiac cycle we chose to model the data as a means of demonstrating those factors in the coronary arterial and venous flow tracings which might be determinants of tissue RBC flux. This model only requires the measured coronary arterial (Q_a) and venous (Q_v) flows and does not need the measured tissue or intramyocardial pressure. The model consisted of two compartments denoting lumped effects of capillaries and venous system having respectively transmural pressures ΔP_c, and ΔP_v volumes V_c and V_v, and compliances C_c and C_v. The resistance to capillary flow into the venous system is regulated by the total cross-sectional area of the capillaries (A_c). Within a finite time interval Δt the rate of capillary flow $\Delta Q_c/\Delta t$ is:

$$\frac{\Delta Q_c}{\Delta t} = G_o \lambda(\Delta P_c)\left\{\left[f_a Q_a / C_c + (1+f_v) Q_v / C_v\right] - Q_c (1/C_c + 1/C_v)\right\},$$

$$\lambda(\Delta P_c) = \left[N(1 + 2\Delta P_c/\alpha)\right]^2 / \eta(t),$$

where f_a is the fraction of Q_a into a regional capillary compartment, f_v is the fraction of Q_v out of the venous compartment, G_o is the capillary patency at $\Delta P_c = 0$. A capillary is considered elastic with a coefficient of α in mmHg, and during ventricular contraction, undergoes shortening defined by a dimensionless function $\eta(t)$[31]. Capillary recruitment due to increase of ΔP_c[32] is also incorporated in the model. Recruitment increases the fraction of the total number of capillaries to be perfused (N) thereby increasing (A_c) and affecting the compliance C_c. The formulation of the above equations and the numerical parameters used to compute the capillary flow Q_c are presented in the Appendix.

Figure 7A shows the measured Q_a, Q_v, the left ventricular pressure and the capillary red cell flux of a canine heart. Figures 7B and 7C depict the computed Q_c based on the measured Q_a and Q_v. Changes in parameters characterizing C_c and C_v results in different capillary flow patterns. The greatest sensitivity for changes in the pattern for microvascular RBC flux arises from changes in C_v. Thus it is possible for a feed-forward control system to exist so that changes in myocardial compression of the intracardiac venous compartment to alter total coronary flow by changing the filling of that compartment.

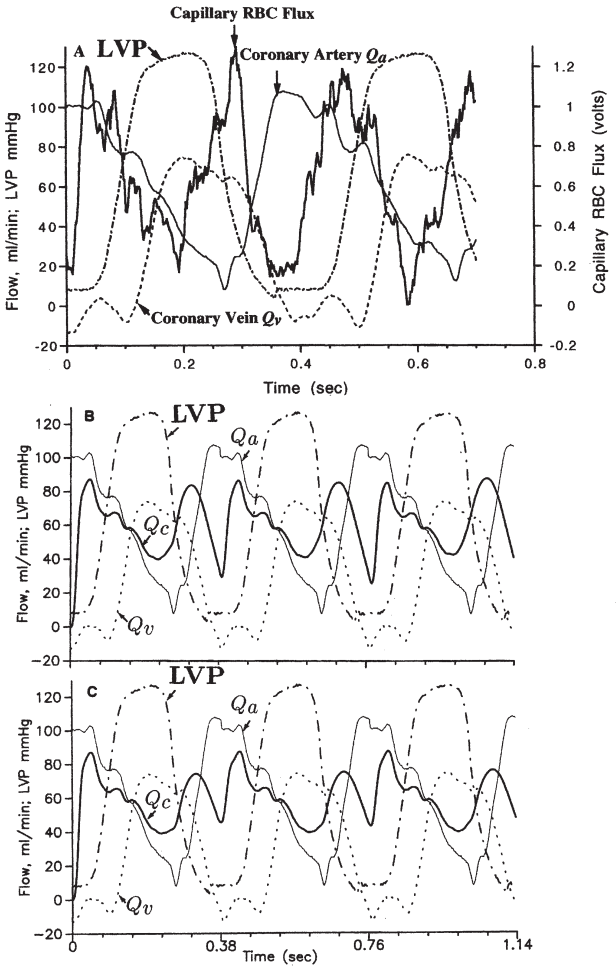

Figure 7. Panel A *demonstrates measured parameters for LVP. Coronary artery flow (Q_a), coronary venous flow (Q_v) and microvascular RBC flux (capillary RBC flux, Q_c) for two cardiac cycles.* Panels B *and* C *display changes in Q_c which result when compliance C_c and C_v are changed in the formulae using measured Q_a and Q_v. Abbreviations as in figure 2.*

In conclusion, we have demonstrated the patterns of RBC flux in some parts of the canine myocardium and have related these observations to techniques used in the past to obtain similar data. Our results confirm that red cell flux in the myocardial superficial microcirculation is mostly continuous but with peaks which relate to coronary events such as coronary arterial inflow, venous outflow and mechanical events such as shape changes of the ventricle. In the endocardium the flux is predominately diastolic. As well, the length of the coronary arterial input and branches may alter the pattern of RBC flux in different parts of the myocardium. Events which primarily alter inflow (stop flow) are modified

and delayed in tissue where the contracting myocyte, collaterals and intramyocardial vascular compliance play important roles. As our device samples a very small area in the myocardium, the representative illustrations should be generalized with caution. It should be recognized that the myocardium is functionally and structurally heterogeneous.

It should be noted that these measurements were performed in an animal with a relatively healthy coronary circulation and may not be extrapolated to responses anticipated in patients with diseased coronary arteries. Similarly, when ischemic or inflammatory induced changes are present involving the supportive collagen network of myocytes[33] tissue responses of RBC flux may be further modified. The challenge now will be using this new technology to explore and understand the microcirculation, which is the major part of the coronary circulation.

Acknowledgments

The authors gratefully acknowledge the support of the Heart and Stroke Foundation of Nova Scotia and the Dalhousie Medical Research Foundation.

Appendix

Within a finite time Δt, the change of V_c and V_v are:

$$\Delta V_c/\Delta t = f_a Q_a - Q_c,\ \Delta P_c = P_c - P_e = V_c/C_c,$$

$$\Delta V_v/\Delta t = Q_c - (1+f_v)\, Q_v,\ \Delta P_v = P_v - P_e = V_v/C_v,$$

where P_e is extravascular pressure. It is assumed that capillary flow is governed by Poiseuille's law:

$$Q_c = \frac{\left[(P_c - P_e) - (P_v - P_e)\right] A_c^2}{8\ \pi\mu L_c},$$

where P_c and P_v are capillary and venous pressures respectively, μ is blood viscosity, A_c and L_c are capillary cross-sectional area and length respectively. Within Δt A_c, L_c, C_c and C_v are considered unchanged. Thus,

$$\frac{\Delta Q_c}{\Delta t} = \frac{A_c^2}{8\ \pi\mu L_c}\left(\frac{\Delta P_c}{\Delta t} - \frac{\Delta P_v}{\Delta t}\right),$$

$$\frac{\Delta P_c}{\Delta t} = \frac{1}{C_c}\frac{\Delta V_c}{\Delta t},\ \frac{\Delta P_v}{\Delta t} = \frac{1}{C_v}\frac{\Delta V_v}{\Delta t}.$$

According to the study of Fibich et al.[31], at a capillary transmural pressure ΔP_c A_c and L_c are:

$$A_c = N(\Delta P_c)\, A_{c,o}\,(1 + 2\Delta P_c/\alpha),\ L_c = L_{c,o}\ \eta(t),$$

where $A_{c,o}$ is the total cross-sectional area of the perfused capillaries at $\Delta P_c = 0$, $L_{c,o}$ is the diastolic capillary length. Therefore,

$$\frac{\Delta Q_c}{\Delta t} = G_o \lambda \left\{\left[f_a Q_a/C_c + (1+f_v)\, Q_v/C_v\right] - Q_c(1/C_c + 1/C_v)\right\},$$

$$G_o = A_{c,o}^2/8\ \pi\mu L_{c,o},\ \lambda = \left[N(1 + 2\Delta P_c/\alpha)\right]^2/\eta(t).$$

$$\eta = 0.9 + 0.2\sin^4(\pi t/T_{cc}),$$

where T_{cc} is the cardiac cycle length.

During diastole the capillary volume and transmural pressure are $V_{c,o}$ and $P_{v,o}$ respectively. The fraction of capillaries (N) increases with ΔP_c according to the following conditions:

$$\Delta P_c - \Delta P_{c,o} < 0,$$

when

$$N = N_o,\ dN/d\Delta P_c = (1 - N_o)k_c,$$

and when

$$N = N_o + (1 - N_o)\left\{(1 - \exp\left[-k_c\,(\Delta P_c - \Delta P_{c,o}\right]\right\}\ dN/d\Delta P_c =$$

$$= (1 - N_o)\, k_c \exp\left[-k_c(\Delta P_c - \Delta P_{c,o})\right]$$

where $\Delta P_{c,o}$ is a critical transmural pressure above which recruitment occurs, N_o is the fraction of the number of capillaries perfused at or below $\Delta P_{c,o}$, and k_c is a constant.

The capillary compliance is:

$$C_c = V_{c,o}\left[2N/\alpha + (1 + 2\Delta P_c/\alpha)\ dN/d\Delta P_c\right].$$

In the venous system the diastolic volume is $V_{v,o}$. When $V_v - V_{v,o} < 0$,

$$\Delta P_v = \Delta P_{v,o} + (V_v - V_{v,o})/C_{v,\max},\ C_v = C_{v,\max},$$

and when $V_v - V_{v,o} > 0$,

$$\Delta P_v = \Delta P_{v,o} + \left\{\exp\left[k_v\,(V_v - V_{v,o} - 1\right]\right\}/(C_{v,\max}\, k_v),$$

$$C_v = C_{v,\max} \exp\left[-k_v\,(V_v - V_{v,o})\right],$$

where $C_{v,\max}$ is the maximal compliance, k_v is a constant.

Numerical parameters. The following numerical parameters were used to compute the capillary flows shown in figure 7: $f_a = 0.95$, $f_v = 0.9$, $G_o = 7.5$ ml/mmHg, $V_{c,o} = 3.2$ ml, $V_{v,o} = 6.0$ ml, $\Delta P_{c,o} = 12$ mmHg, $\Delta P_{v,o} = 5$ mmHg, $\alpha = 800$ mmHg, $k_c = 1.0$ mmHg^{-1}, $N_o = 0.75$. The diastolic $\Delta P_c = 12.0$ mmHg. In figure 7B, $k_v = 6.0$ ml^{-1}, $C_{v,\max} = 0.25$ ml/mmHg, and in figure 7C, $k_v = 2.0$ ml^{-1}, $C_{v,\max} = 0.175$ ml/mmHg.

References

1. Chilian WM. Coronary microcirculation in health and disease. Summary of an NHLBI Workshop. Circulation 1997; 95: 522-8.
2. Hellberg K, Wayland H, Rickart AL, Bing RJ. Studies on the coronary microcirculation by direct visualization. Am J Cardiol 1972; 29: 593-7.
3. Tillmanns H, Ikeda S, Hansen H, Sarma JSM, Fauvel JM, Bing RJ. Microcirculation in the ventricle of the dog and turtle. Circ Res 1974; 34: 561-9.
4. Ashikawa K, Kanatsuka H, Suzuki T, Takishima T. Phasic blood flow velocity pattern in epimyocardial microvessels in the beating canine left ventricle. Circ Res 1986; 59: 704-11.

5. Yada T, Hiramatsu O, Kimura A, et al. Direct in vivo observation of subendocardial arteriolar responses during reactive hyperemia. Circ Res 1995; 77: 622-31.
6. Nellis SH, Liedtke AJ, Whitesell L. Small coronary vessel pressure and diameter in an intact beating rabbit heart using fixed-position and free-motion techniques. Circ Res 1981; 49: 342-53.
7. Klassen GA, Barclay KD, Wong R, Paton B, Wong AYK. Red cell flux during the cardiac cycle in the rabbit myocardial microcirculation. Cardiovasc Res 1997; 34: 504-14.
8. Mito K. Characteristics of laser Doppler flowmeters with differing optical arrangements. J Med Eng Technol 1992; 16: 236-42.
9. Schemitsch EH, Kowalski MJ, Swiontkowski MF. Evaluation of a laser Doppler flowmetry implantable fiber system for determination of threshold thickness for flow detection in bone. Calcif Tissue Int 1994; 55: 216-22.
10. Kirkeby OJ, Rise IR, Nordsletten L, Skjeldal S, Hall C, Risöe C. Cerebral blood flow measured with intracerebral laser-Doppler flow probes and radioactive microspheres. J Appl Physiol 1995; 79: 1479-86.
11. Gregg DE. Coronary circulation in health and disease. Philadelphia, PA: Lea & Febiger, 1950.
12. Ahn HC, Ekroth R, Hedenmark J, Nilsson GE, Svedjeholm R. Assessment of myocardial perfusion in the empty beating porcine heart with laser Doppler flowmetry. Cardiovasc Res 1988; 22: 719-25.
13. Ahn HC, Ekroth R, Nilsson GE, Svedjeholm R, Thelin S. Laser Doppler flowmetry estimating myocardial perfusion after internal mammary artery grafting. Scand J Thorac Cardiovasc Surg 1988; 22: 281-4.
14. Buckberg GD, Fixler DE, Archie JP, Hoffman JIE. Experimental subendocardial ischemia in dogs with normal coronary arteries. Circ Res 1972; 30: 67-81.
15. Arts T, Meerbaum S, Reneman RS, Corday E. Torsion of the left ventricle during the ejection phase in the intact dog. Cardiovasc Res 1984; 18: 183-93.
16. Zamir M. Distributing and delivering vessels of the human heart. J Gen Physiol 1988; 91: 725-35.
17. Chilian WM, Marcus ML. Effects of coronary and extravascular pressure on intramyocardial and epicardial blood velocity. Am J Physiol 1985; 248: H170-H178.
18. Kajiya F, Tsujioka K, Ogasawara Y, et al. Analysis of the characteristics of the flow velocity waveforms in left atrial small arteries and veins in the dog. Circ Res 1989; 65: 1172-81.
19. Taylor JR, Taylor AJ. The relationship between the sinus node and the right atrial appendage. Can J Cardiol 1997; 13: 85-92.
20. Mildenberger RR, L'Abbate A, Zborowska-Sluis DT, Klassen GA. The relationship between oxygen extraction and extravascular mean transit time in the canine heart. Can J Physiol Pharmacol 1977; 55: 478-81.
21. Kuznetsova LV, Tomasek N, Sigurdsson GH, Banic A, Erni D, Wheatley AM. Dissociation between volume blood flow and laser-Doppler signal from rat muscle during changes in vascular tone. Am J Physiol 1998; 274: H1248-H1254.
22. Klassen GA. The coronary circulation: Quo vadis. Cardiologia 1999; 44: 699-710.
23. Helmke BP, Bremner SN, Zweifach BW, Skalak R, Schmid-Schönbein GW. Mechanisms for increased blood flow resistance due to leukocytes. Am J Physiol 1997; 273: H2884-H2890.
24. Olsson RA. Myocardial reactive hyperemia. Circ Res 1975; 37: 263-70.
25. Marcus M, Winniford MD, Rossen JD. Coronary reserve in the human coronary circulation. In: Kajiya F, Klassen GA, Spaan JAE, Hoffman JIE, eds. Coronary circulation. Basic mechanisms and clinical relevance. Tokyo: Springer-Verlag, 1990: 281-94.
26. Schaper W. The collateral circulation of the heart. Amsterdam: North-Holland Publishing Company, 1971.
27. Spaan JA, Cornelissen AJ, Chan C, Dankelman J, Yin FC. Dynamics of flow, resistance, and intramural vascular volume in canine coronary circulation. Am J Physiol 2000; 278: H383-H403.
28. Klassen GA, Agarwal JB, Tanser PH, Woodhouse SP, Marpole D. Blood flow and tissue space of the left coronary artery in man. Circ Res 1970; 27: 185-95.
29. Ruiter JH, Spaan JAE, Laird JP. Transient oxygen uptake during myocardial reactive hyperemia in the dog. Am J Physiol 1977; 232: H437-H440.
30. Sestier FJ, Mildenberger RR, Klassen GA. Role of autoregulation in spatial and temporal perfusion heterogeneity of the canine myocardium. Am J Physiol 1978; 235: H64-H71.
31. Fibich G, Lanir Y, Liron N. Mathematical model of blood flow in a coronary capillary. Am J Physiol 1993; 265: H1829-H1840.
32. Chadwick RS, Tedgui A, Michel JB, Ohayon J, Levy BI. Phasic regional myocardial inflow and outflow: comparison of theory and experiments. Am J Physiol 1990; 258: H1687-H1698.
33. Depré C, Vanoverschelde JLJ, Melin JA, et al. Structural and metabolic correlates of the reversibility of chronic left ventricular ischemic dysfunction in humans. Am J Physiol 1995; 268: H1265-H1275.